Chin. J. Astron. Astrophys. Vol. 7 (2007), No. 6, 803–808
(*http://www.chjaa.org*)

Chinese Journal of
Astronomy and
Astrophysics

Generation of Interstellar Class II 7_2–8_1A$^+$ and 7_2–8_1A$^-$ Methanol Masers *

Han-Ping Liu[1] and Jin Sun[2]

[1] Department of Physics, Beijing Normal University, Beijing 100875; *gaozm@bnu.edu.cn*
[2] Department of Astronomy, Beijing Normal University, Beijing 100875

Received 2007 March 9; accepted 2007 July 17

Abstract New methanol maser lines at $7_2 \rightarrow 6_3$A$^-$(86.6 GHz) and $7_2 \rightarrow 6_3$A$^+$(86.9 GHz) together with two candidate methanol maser lines at $7_2 \rightarrow 8_1$A$^-$(80.99 GHz) and $7_2 \rightarrow 8_1$A$^+$(111.29 GHz) have been detected in W3(OH). We use a pumping mechanism, i.e., methanol masers without population inversion, to explain the formation of weak methanol masers of $7_2 \rightarrow 8_1$A$^+$ and $7_2 \rightarrow 8_1$A$^-$. We explain well why the line-shape of the transition $7_2 \rightarrow 8_1$A$^+$ is not typical. A similar argument can be applied to the Λ-type level system 7_2A$^-$, 6_3A$^-$ and 8_1A$^-$, as well as to the $7_2 \rightarrow 8_1$A$^-$ 80.99 GHz masers.

Key words: pumping mechanism — Class II methanol sources — maser without inversion — coherent microwave field

1 INTRODUCTION

Interstellar methanol molecular emissions were first seen in 1971 (Barrett et al. 1971), and it took several years for their status as masers was established (Chui et al. 1974; Hills et al. 1975). To date, approximately 30 maser transitions of methanol have been observed. The methanol masers can be divided into two distinctive classes (Batrla et al. 1987; Menten 1991). Class I methanol masers are typically well separated from strong embedded stellar objects, ultra-compact HII (UC HII) regions and OH masers. Class II methanol masers, on the other hand, are found in close association with massive star formation regions, making them a useful signpost of such regions. In no case does a Class I methanol maser emit a Class II maser line, and vice versa. Sobolev (1993) has proposed further subdivisions of these two main Classes.

There is considerable evidence that many of the class II methanol masers are located in the same regions of space (Sutton et al. 2001). The physical parameters are generally consistent with those determined from observations of massive star formation regions (Cragg et al. 2001). A star-forming region, W3(OH), at a distance of about 2.2 kpc, is a prototype Class II methanol maser source: it contains an expanding UC-HII region surrounding a young O7 star. Almost all known Class II maser lines have been found in W3(OH), such as the strongest 6.7 and 12.2 GHz masers, and the relatively weaker ones at 29, 86 and 38 GHz, etc. It has been shown that the Class II methanol maser phenomenon is very widespread. Detailed studies of masers in various transitions will help understand their nature.

One of the major goals in the investigation of astrophysical masers is to better understand the maser pumping mechanism, especially for the Class II methanol masers, but this topic is still under debate. To search the physical characteristics of the masing material in the region W3(OH), Sutton et al. (2001) have carried out additional masing transitions in W3(OH) with the BIMA 10-element interferometer. In their paper, the transitions 7_2–6_3A$^\pm$ at 86.9 and 86.6 GHz were observed and classified as Class II methanol masers. Transitions 7_2–8_1A$^\pm$ at 111 and 81 GHz also were detected (Sutton et al. 2001) and found to have

* Supported by the National Natural Science Foundation of China.

a pedestal line shape, indicating either quasi-thermal emission or a blend of weak maser features. Sutton et al. (2001) demonstrated that these pedestal lines within the region W3(OH) are weak masers, arising from material with physical characteristics similar to that giving rise to the stronger methanol masers. Furthermore, these two sets of maser lines of 7_2–6_3A$^{\pm}$ and 7_2–8_1A$^{\pm}$ are basically coincident, but their morphology are different. Their high excitation energy masing levels can provide powerful constraints on the pumping mechanism.

In this paper we will use a pumping mechanism (see Imamoglu et al. 1991; Agarwal 1991; Liu et al. 1998, 2002a,b) for the interstellar 7_2–8_1A$^{\pm}$ methanol masers, but without considering the origin of the 7_2–6_3A$^{\pm}$ masers, because the mechanism can interpret well the formation and behavior of Class II 7_2–8_1A$^{\pm}$ methanol masers.

2 THE PUMPING OF CLASS II METHANOL 7_2–8_1A$^{\pm}$ MASERS

2.1 The Principle of Maser without Population Inversion

There has been considerable interest recently in the study of lasing without the requirement of population inversion. Several schemes have been proposed. One is the Λ-type three-level system with coherent pumping (Imamoglu et al. 1991; Agarwal 1991). As shown in Figure 1, a three-level system has levels of |a>, |b> and |c> , each with energies 0, $\hbar\omega_{\rm ab}$ and $\hbar\omega_{\rm ac}$, respectively, γ_1 (γ_2) is the spontaneous decay rate from state |c> to state |a> (|b>), $\lambda_1(\lambda_2)$ is the incoherently pumping rate by thermal radiation. From Figure 1 there is no direct dipole coupling between states |a> and |b>. The transition |b>–|c> with frequency $\omega_{\rm bc}$ is driven by a strong coherent field of frequency ω_2 with Rabi frequency $2G$, we set $\Delta_2 = \omega_{\rm bc} - \omega_2$ and $G = E_{20}|\rho_{\rm bc}|\pi/\hbar$, where E_{20} is the amplitude of strong coherent field, $\rho_{\rm bc}$ is the dipole transition matrix element. A probe field with frequency ω_1 (Rabi frequency $2g$) is applied to the transition |a>–|c> with frequency $\omega_{\rm ac}$. We also set $\Delta_1 = \omega_{\rm ac} - \omega_1$and both G and g to be positive for simplicity.

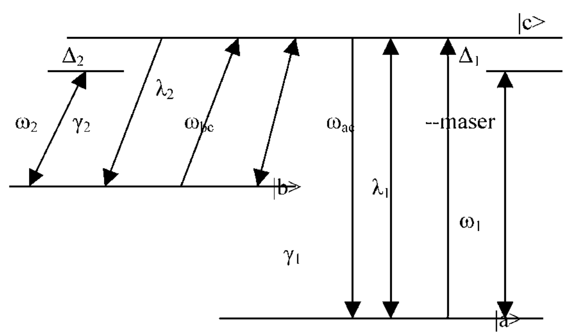

Fig. 1 Λ-type three-level system with coherent pumping.

Time-dependent equations for the particle density matrix in the rotating frame can be written as:

$$\begin{aligned} d\rho_{\rm aa}/dt &= \gamma_1\rho_{\rm cc} - \lambda_1\rho_{aa} + ig(\rho_{\rm ca} - \rho_{\rm ac}), \\ d\rho_{\rm bb}/dt &= \gamma_2\rho_{\rm cc} - \lambda_2\rho_{\rm bb} + iG(\rho_{\rm cb} - \rho_{\rm bc}), \\ d\rho_{\rm cc}/dt &= -(\gamma_1+\gamma_2)\rho_{\rm cc} + \lambda_1\rho_{\rm aa} + \lambda_2\rho_{\rm bb} + iG(\rho_{\rm bc} - \rho_{\rm cb}) + ig(\rho_{\rm ac} - \rho_{\rm ca}), \\ d\rho_{ab}/dt &= -(\lambda_{12} - i\Delta\omega_{21})\rho_{\rm ab} - iG\rho_{\rm ac} + ig\rho_{\rm cb}, \\ d\rho_{\rm ac}/dt &= -(\gamma_{13} - i\Delta\omega_{31})\rho_{\rm ac} + ig(\rho_{\rm cc} - \rho_{\rm aa}) - iG\rho_{\rm ab}, \\ d\rho_{\rm bc}/dt &= -[\gamma_{23} - i(\Delta\omega_{31} - \Delta\omega_{21})]\rho_{\rm bc} + iG(\rho_{\rm cc} - \rho_{\rm bb}) - ig\rho_{ba}, \end{aligned} \tag{1}$$

where $\lambda_{12} = (\lambda_1+\lambda_2)/2$, $\gamma_{13} = (\gamma_2+\lambda_2+2\lambda_1+\gamma_1)/2$, $\gamma_{23} = (\gamma_2+2\lambda_2+\lambda_1+\gamma_1)/2$, $\Delta\omega_{21} = \omega_{\rm ab}+\omega_2-\omega_1$ and $\Delta\omega_{31} = \omega_{\rm ac}-\omega_1$.

For simplicity, the time-dependent density matrix Equations (1) can be solved in the steady state, and the imaginary component of the density matrix element $\rho_{\rm ac}$, for instance, can be described as (the higher order terms of g being negligibly tiny):

$$\begin{aligned}\mathrm{Im}(\rho_{\mathrm{ac}}) \;=\; &(\lambda_{12}\gamma_{13}+\Delta\omega_{21}\Delta\omega_{31})gG[fG^2(\rho_{\mathrm{aa}}-\rho_{\mathrm{cc}})-a\gamma_2\rho_{\mathrm{bb}}/2]/\\ &[(G^2+\lambda_{12}\gamma_{13}-\Delta\omega_{21}\Delta\omega_{31})^2+(\lambda_{12}\Delta\omega_{31}+\gamma_{13}\Delta\omega_{21})^2]ja,\end{aligned} \tag{2}$$

where we set $f=(\lambda_1+\gamma_2)/\,2$, $a=\Delta_2^2+f^2$, $d=f+\gamma_1/2$, $j=\lambda_1+\gamma_1/2$.

The time-dependent equation for the probe field amplitude E_{10} can be written as

$$dE_{10}/dt=-kE_{10}-2\pi i\omega_1 Np_{\mathrm{ca}}\times\rho_{\mathrm{ac}}, \tag{3}$$

where k is the loss rate of propagation, N the number density of molecules, and ρ_{ca} the matrix element of dipole transition. If k is tiny enough, we can just consider the second component of Equation (3). Since the imaginary component of the density matrix element ρ_{ac} is positive, $dE_{10}/dt>0$ and then the probe field E_{10} is amplified in the course of time.

Based on the quantum coherent effect, the spontaneous emission from the upper state |c> to the lower state |a> will be restrained, while the stimulated emission is not affected significantly. Then, even if there is no population inversion between the upper and lower levels, a net coherent light amplification –laser (or maser) always exists. Thus, the strong coherent field acts as a trigger or a stimulant.

It is worth noting that Im(ρ_{ac})>0 is a basic requirement to produce amplification of the coherent radiation. In order to explain the observed maser intensities in detail, large gain coefficients and appropriate interstellar conditions regarding the gas density and coherent path length of maser region are needed.

2.2 The Relevant Level Structure of Methanol Molecule

Methanol is one of the simplest molecules displaying hindered internal rotation. It is also a slightly asymmetric top, for the OH group does not lie on the principal molecular axis. As a general description, the energy levels of the methanol molecule share the same quantum numbers but J can be expanded into a Taylor series in $J(J+1)$ (Ioli et al. 1995):

$$E(q,J)=\Sigma a_m(q)[J(J+1)]^m\pm[(J+K)!/2(J-K)!][S(q)+J(J+1)T(q)], \tag{4}$$

where q stands for the conventional quantum numbers in the sequence, v, n, τ, K, with v standing for the vibrational quantum number, n the torsional vibration quantum number, τ may have the values 1, 2 and 3, and arises from the threefold nature of the hindering potential. J is the total angular momentum quantum number, and the projection of K is along the internal axis. Since the frequencies corresponding to pure vibrational modes are of the order of 1000 cm^{-1}, only the ground level ($v=0$) is of interest here. It is worth pointing out that transitions may only occur between states belonging to the same symmetry species — A or E. The term including S and T describes the asymmetry doubling, designated by + or –, and is present only for levels belonging to A symmetry with small but nonzero K values. The sum in Equation (4) can be truncated at $m=4$, but $m=3$ is sufficient in some cases and $m=5$ is needed in other cases. In this section we are only interested in the transition of 7_2–6_3A$^\pm$ and 7_2–8_1A$^\pm$, $v=0$, $n=0$. The latest relevant parameters can be found in Moruzzi et al. (2000).

The appropriate selection rules are:

$$\begin{aligned}&+\;\rightarrow\;+\;\text{ and }\;-\rightarrow-,\;\text{ for }\;\Delta J=\pm1,\quad \Delta n=0;\\ &+\;\rightarrow\;-\;\text{ and }\;-\rightarrow+,\;\text{ for }\;\Delta J=0,\quad \Delta n=0.\end{aligned}$$

Accordingly, level 7_2A$^+$ can transit to levels of 6_3A$^+$and 8_1A$^+$. As shown in Figure 2, the three levels, 7_2A$^+$, 6_3A$^+$ and 8_1A$^+$, form a Λ-type three-level system. Similarly, 7_2A$^-$, 6_3A$^-$ and 8_1A$^-$ form another Λ-type three-level system. Two Λ-type three-level systems with coherent pumping can generate masers without the need of population inversion.

2.3 The Pumping of Class II 7_2–8_1A$^+$ and 7_2–8_1A$^-$ Methanol Masers

In this section, we argue that the 7_2–8_1A$^+$ 111 GHz methanol masers are that without inversion driven by the interstellar 7_2–6_3A$^+$ 86.9 GHz methanol masers, without considering the origin of the last. From our result, the 7_2–8_1A$^+$ and 7_2–6_3A$^+$ transitions share a same upper level, 7_2A$^+$ level and 7_2–6_3A$^+$ at

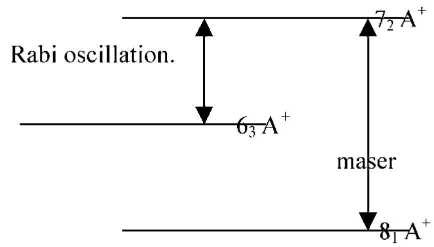

Fig. 2 A set of Λ-type three-level system for methanol.

86.9 GHz line show maser emission. It would be reasonable to expect maser transition for 7_2–8_1A$^+$ at 111 GHz.

Sutton et al. (2001) have carried out a deep search of W3(OH) using the BIMA 10-element interferometer. The phase center of the mapping observation is $\alpha(\mathrm{J2000}) = 2^{\mathrm{h}}27^{\mathrm{m}}03.87^{\mathrm{s}}$, $\delta(\mathrm{J2000}) = 61°52'24.6''$, the spatial resolution is of the order of $1.5''$–$2.5''$, and the positional accuracy, of the order of $0''.1$. Nine transitions of methanol have been detected by Sutton et al. (2001). All the nine lines show a pedestal line shape, and three of them, 7_2–6_3A$^\pm$ and 3_1–4_0A$^+$, exhibit the "spike + pedestal" line shape. The latter three transitions undoubtedly belong to maser emission. Furthermore, Sutton et al. (2001) have demonstrated that the pedestal line-shape emissions, for instance 7_2–8_1A$^\pm$, are weak maser action, and come from a blend of maser features. The spike component of the transition 7_2–6_3A$^+$ is located $0.6''$ north and $0.2''$ west of the center of our map. The peak is at $v_{\mathrm{LSR}} = -43.1\,\mathrm{km\ s^{-1}}$. The transition 7_2–8_1A$^+$ shows a pedestal line shape with a peak at $v_{\mathrm{LSR}} = -43.2\,\mathrm{km\ s^{-1}}$, and roughly coincides with the 7_2–6_3A$^+$ transition position and velocity within the uncertainties.

According to the selection rules the levels, 7_2^+, 6_3^+ and 8_1^+ can constitute a Λ-type three level system, which can produce masers without inversion. For the 7_2–6_3A$^+$ 86.9 GHz maser emission, the peak flux density in the spike component is 7.2 Jy, and the total integrated flux is 11.2 Jy km s^{-1}, corresponding to 3.253×10^6 Jy Hz. The distance from W3(OH) to the Earth, $D = 2.2\,\mathrm{kpc}$, and the size of the source is $d \approx 0.1'' \approx 5 \times 10^{14}\,\mathrm{cm}$ (200 AU) at 2.2 kpc. This is within the range presented by Slysh et al. (1999). Therefore, the energy flux density of source region will be $S = (3.253 \times 10^6 \times 10^{-26}\,\mathrm{W\ m^{-2}}) \times (D/d)^2 = 5.993 \times 10^{-6}\,\mathrm{W\ m^{-2}}$ and the energy density in the maser source region is $w = S/c = 1.998 \times 10^{-14}\,\mathrm{J\ m^{-3}}$ (c the light speed). Then, we can calculate the electric field E though $w = \varepsilon_0\langle E^2\rangle/2 = \varepsilon_0 E_{20}^2/4 \rightarrow E_{20} = (4w\varepsilon_0)^{1/2} = 9.503 \times 10^{-2} N\,\mathrm{C}^{-1}$, where E_{20} is amplitude of electric strength, $\varepsilon_0 = 8.85 \times 10^{-12}\mathrm{C}^2 N^{-1}\mathrm{m}^{-2}$ is dielectric constant. We assume ρ_{bc} of $CH_3OH \approx 1$ Debye (Xu et al. 1997a) and in general the size of the central star $r \approx 10^{13}$ cm. With these parameters assumed or calculated, we have the Rabi frequency $G = 4.5252 \times 10^3\,\mathrm{s^{-1}}$.

According to quantum mechanics, the incoherently pumping rate by the thermal radiation is

$$\lambda = B \cdot w(\omega) = A/[\exp(-\hbar\omega/kT) - 1], \tag{5}$$

where $w(\omega)$ is radiative energy density with frequency ω (caused by dust). The radiation temperature of dust can be estimated to be 175 K (Sutton et al. 2001). The Einstein coefficient A of transition 7_2–6_3A$^+$ is $6.540 \times 10^{-7}\,\mathrm{s^{-1}}$ (Pei et al. 1988), and the transition frequency 86.9029 GHz (Xu et al. 1997b). For transition 7_2–8_1A$^+$, A=$2.453 \times 10^{-6}\,\mathrm{s^{-1}}$, and $\omega = 111.2896$ GHz, for transition 7_2–8_1A$^+$. Thus, we have $\lambda_1 = 7.9067 \times 10^{-5}\,\mathrm{s^{-1}}$ and $\lambda_2 = 2.7087 \times 10^{-5}\,\mathrm{s^{-1}}$ from Equation (5), and then we have $\lambda_{12} = 5.3077 \times 10^{-5}\,\mathrm{s^{-1}}$, $\gamma_{13} = 1.4445 \times 10^{-4}\,\mathrm{s^{-1}}$ and $\gamma_{23} = 1.2254 \times 10^{-4}\,\mathrm{s^{-1}}$. In the case of resonance for Equation (5), we can have $f = 4.076 \times 10^{-5}\,\mathrm{s^{-1}}$, $a = 1.661 \times 10^{-9}\,\mathrm{s^{-2}}$, $d = 4.19866 \times 10^{-5}\,\mathrm{s^{-1}}$ and $j = 8.02935 \times 10^{-5}\,\mathrm{s^{-1}}$. With parameters calculated, one can obtain $\mathrm{Im}(\rho_{\mathrm{ac}}) = 3.4695 \times 10^{-5} g \times [18.445(\rho_{\mathrm{aa}}–\rho_{\mathrm{cc}})–5.4315 \times 10^{-16}\rho_{\mathrm{bb}}]/55.92$. It is given that $\rho_{\mathrm{aa}}–\rho_{\mathrm{cc}} > 0$ and $\rho_{\mathrm{aa}} - \rho_{\mathrm{cc}} > \rho_{\mathrm{bb}}$ with $\rho_{\mathrm{aa}} - \rho_{\mathrm{cc}}$ is far larger than ρ_{bb}. Therefore, we derive $\mathrm{Im}(\rho_{\mathrm{ac}}) > 0$ which introduces a coherent amplification between states $|c>$ and |a>. Levels of 7_2^+, 6_3^+ and 8_1^+ together constitute a typical three-level system with coherently pumping and introduce masers without the need of inversion. The $7_2 \rightarrow 8_1$A$^+$ 111.3 GHz maser is associated with $7_2 \rightarrow 6_3$A$^+$ 86.9 GHz maser.

For Class II 7_2–8_1A$^-$ methanol masers, the levels 7_2A$^-$, 6_3A$^-$ and 8_1A$^-$ constitute another Λ-type three level system, driven by 7_2–6_3A$^-$ 86.6 GHz masers (same process as in Fig. 2). The Einstein coefficient A of the transition 7_2–6_3A$^-$ is $5.476 \times 10^{-7}\,\mathrm{s}^{-1}$ (Pei et al. 1988), and the transition frequency equals 86.6156 GHz (Xu et al. 1997b). For transition 7_2–8_1A$^-$, we have $A = 9.454 \times 10^{-7}\,\mathrm{s}^{-1}$, the frequency is 80.9933 GHz. These two maser transitions share a same upper level 7_2A$^-$. According to Sutton (2001), the peak flux density in the spike component of 7_2–6_3A$^-$ masers is 6.7 Jy, and the total integrated flux is 11 Jy km s^{-1}, which corresponds to 3.1759×10^6 Jy Hz. The distance of W3(OH), $D \approx 2.2$ kpc, and a source size of $d \approx 5\times10^{14}$ cm. Therefore, the energy flux density of the source region will be S' (the calculation below is similar to Section 2.2, thus we mark the corresponding quantities by an apostrophe):

$$\begin{aligned}
S' &= (3.1759 \times 10^6 \times 10^{-26}\,\mathrm{W\,m^{-2}}) \times (D/d)^2 = 5.851 \times 10^{-6}\,\mathrm{W\,m^{-2}},\\
W' &= S'/c = 1.951 \times 10^{-14}\,\mathrm{J\,m^{-3}},\\
E'_{20} &= (4w/\varepsilon_0)^{1/2} = 8.818 \times 10^{-3} N\,C^{-1},\\
G' &= 4.199 \times 10^2\,\mathrm{s^{-1}},\\
\lambda'_1 &= 4.2047 \times 10^{-5}\,\mathrm{s^{-1}},\\
\lambda'_2 &= 2.2756 \times 10^{-5}\,\mathrm{s^{-1}},\\
\lambda'_{12} &= 3.24015 \times 10^{-5}\,\mathrm{s^{-1}},\\
\gamma'_{13} &= 5.41715 \times 10^{-5}\,\mathrm{s^{-1}},\\
\gamma'_{23} &= 4.4526 \times 10^{-5}\,\mathrm{s^{-1}},\\
f' &= 2.12973 \times 10^{-5}\,\mathrm{s^{-1}},\\
a' &= 4.5357 \times 10^{-10}\,\mathrm{s^{-2}},\\
d' &= 2.177 \times 10^{-5}\,\mathrm{s^{-1}},\\
j' &= 4.25179 \times 10^{-5}\,\mathrm{s^{-1}}
\end{aligned}$$

and

$$\mathrm{Im}(\rho'_{\mathrm{ac}}) = 7.3701 \times 10^{-7} g[3.7551(\rho'_{\mathrm{aa}} - \rho'_{\mathrm{cc}}) - 1.24187 \times 10^{-16}\rho'_{\mathrm{bb}}]/5.9957 \times 10^{-4} > 0\,.$$

Also, the levels 7_2^-, 6_3^- and 8_1^- together constitute a typical three-level system with coherently pumping and result in masers without the need of population inversion.

3 DISCUSSION

Maser emission from interstellar methanol is observed toward many dense molecular cloud cores in regions of massive star formation. The search for new methanol maser transitions is still in progress. Methanol masers are observed in transitions between energy levels in different K ladders. The pumping mechanisms of the two classes of methanol masers have not been well understood so far, though the collision mechanism seems proper for the Class I sources (Walmsley et al. 1988). We note that for A-species levels of methanol, the lowest level has quantum numbers of $J = 1$, $K = 0$. A strongly preferential process is $\Delta K = 0$ for collision excitation (Lees et al. 1974), that can become the population inversion mechanism for $J_0 \rightarrow (J-1)_1$A$^+$ masers, such as the $7_0 \rightarrow 6_1$A$^+$, $8_0 \rightarrow 7_1$A$^+$, and $9_0 \rightarrow 8_1$A$^+$ masers at 44, 95 and 146 GHz, respectively. This mechanism also produces enhanced absorption in the 107 GHz of $3_1 \leftarrow 4_0$A$^+$ transition and 6.7 GHz of $5_1 \leftarrow 6_0$A$^+$ transition toward Class I sources which is the character of Class I, but in Class II masers the situation is reversed: the $3_1 \rightarrow 4_0$A$^+$ and $5_1 \rightarrow 6_0$A$^+$ transitions present strong maser emissions toward Class II methanol sources. That cannot be explained at all by the collision mechanism.

We propose that the pumping mechanism and physical conditions of these two classes of methanol masers in the region W3(OH) may be different from each other. In the W3(OH) region, radiative processes are likely to be a main source of pumping energy for Class II methanol masers. In that region, the strong thermal emission of the central star and dust will populate the excitation levels of the methanol molecule and the $7_2 \rightarrow 6_3$A$^+$ and $7_2 \rightarrow 8_1$A$^+$ masers are closely associated with each other. The levels 7_2A$^+$, 6_3A$^+$ and 8_1A$^+$constitute a typical three-level system with coherently pumping. Since the strong coherent driving of $7_2 \rightarrow 6_3$A$^+$ masers as a trigger, the transition $7_2 \rightarrow 8_1$A$^+$ generates masers without inversion.

Therefore, one can understand why the line-shape of the transition $7_2 \rightarrow 8_1A^+$ is not typical spiky. A similar argument can be offered to the Λ-type level system 7_2A^-, 6_3 A^- and 8_1A^-, as well as the 7_2–8_1A^- 80.99 GHz masers. Since for the various environments of maser forming regions, different mechanisms are proposed to explain the masers in some detail, the nature of the pumping mechanism is still under debate.

Acknowledgements The authors gratefully acknowledge the financial support of National Natural Science Foundation of China (Nos. 19873003 and 20073005).

References

Agarwal G. S., 1991, Phys. Rev. A44, R28
Barrett A. H., Schwartz P. R., Waters J. W., 1971, ApJ, 168, L101
Batrla W. et al., 1987, Nature, 326, 49
Chui M. F., Cheung A. C., Matsakis D. et al., 1974, ApJ, 187, L19
Cragg D. M. et al., 2001, MNRAS, 323, 939
Hills R., Pankonin V., Landecker T. L., 1975, A&A, 39, 149
Imamoglu A., Field J. F., Harris S. E., 1991, Phys. Rev. Lett., 66, 1154
Ioli N. et al., 1995, J. Mol. Spectrosc, 171, 130
Lees R. M., Hague S. S., 1974, Can. J. Phys., 52, 2250
Liu H., Sun J., 1998, Optics Comm., 150, 153
Liu H., Sun J., Thissen T., 2002a, Ap&SS, 279, 367
Liu H., Sun J., 2002b, Chin. J. Astron. Astrophys. (ChJAA), 2, 51
Menten K. M.:1991, in: A.D.Haschick & P.T.P.Ho (eds.), Skylines, Proc. Third Haystack, Observatory Meeting, ASP, San Francisco, p.119
Moruzzi G., Winnewisser B. P., Winnewisser M., 2000, Microwave, Infrared, and Laser Transitions of Methanol, CRC Press, Inc., New York
Pei C. C., Gou Q. Q., Zeng Q., 1988, A&AS, 76, 35
Slysh V. I., Val'tts I. E., Kalenskii S. V., Larionov V. V., 1999, Astron. Rep., 43, 657
Sobolev A. M., 1993, Astron. Lett., 19, 293
Sutton E. C., Sobolev A. M., Ellingsen S. P. et al., 2001, ApJ, 554, 173
Walmsley C. M. et al., 1988, A&A, 197, 271
Xu L. H., Lovas F. L., 1997a, J. Phys. Chem. Ref. Data, 26, 22
Xu L. H., Lovas F. L., 1997b, J. Phys. Chem. Ref. Data, 26, 29